ARTICLE IN PRESS

Available online at www.sciencedirect.com

ScienceDirect

Advances in Space Research xxx (xxxx) xxx

ELSEVIER

ADVANCES IN SPACE RESEARCH (a COSPAR publication)

www.elsevier.com/locate/asr

The cosmic-ray spectrum in the PeV to EeV energy range

Donghwa Kang*, Andreas Haungs

Karlsruhe Institute of Technology, Institute for Astroparticle Physics, Karlsruhe 76021, Germany

Received 15 January 2024; received in revised form 18 June 2024; accepted 20 June 2024

Abstract

Cosmic rays around the so-called knee in the spectrum at around PeV primary energy are generally galactic in origin. Observations on the form of their energy spectrum and their mass composition are fundamental tools to understand the origin, acceleration and propagation mechanism of high-energy cosmic rays. In addition, it is required to find signatures to clarify the transition from galactic to extragalactic sources, which are believed to be responsible for the highest-energy cosmic rays above EeV. This brief review focuses on recent experimental results around the knee of the all-particle energy spectrum and composition in the energy range of the knee up to EeV energies.

Keywords: Cosmic rays; Energy spectrum; Mass composition; Extensive air-showers

1. Introduction

Studying high-energy cosmic rays have been performed to find their sources since their discovery nearly a century ago. However, the origin of cosmic rays and their propagation mechanism are not completely understood yet. The goal of experimental cosmic-ray studies is to determine the energy spectrum, mass composition and the arrival direction of cosmic rays. The energy spectrum of primary cosmic rays reveals some characteristic features, which hold information about the origin, acceleration and mass composition.

The all-particle energy spectrum of cosmic rays, in general, follows a power law ($dN/dE \propto E^{\gamma}$) with a spectral index of γ around -3. Cosmic rays up to the energy of about 10^{14} eV can be measured directly by balloon or satellite experiments, whereas for higher energies direct measurements cannot provide data with sufficient statistics due to their small sensitive detection area and exposure time. Experiments thus have to observe the cosmic rays above 10^{14} eV indirectly by measuring extensive air showers (Haungs et al., 2003).

Above 10^{15} eV, the all-particle spectrum has a power-law-like behavior with $\gamma \sim -2.7$. The prominent feature is known as the knee around $3 - 5 \times 10^{15}$ eV, where the spectral index changes from about -2.7 to -3.1. The general explanation of the steepening of the spectrum is due to the breakdown of galactic acceleration mechanisms of the cosmic rays (Hillas, 2005), first of the lowest charges, so that the energy positions of the knees for different cosmic ray primaries would be expected to depend on their atomic number.

In addition, propagation of cosmic rays is charge-dependent. Cosmic rays which undergo faster diffusion will escape more easily from the Galaxy and eventually leads to less flux observed at the Earth. Depending on escaping the sources, the charged particles diffuse in random magnetic field that count for their relatively long confinement time in the Galaxy. The diffusion model probably works for particles with energies not much larger than $10^{17} \cdot Z$ eV, where Z is the particle charge.

* Corresponding author.
E-mail addresses: donghwa.kang@kit.edu (D. Kang), andreas.haungs@kit.edu (A. Haungs).

https://doi.org/10.1016/j.asr.2024.06.053
0273-1177/© 2024 Published by Elsevier B.V. on behalf of COSPAR.

Please cite this article as: D. Kang and A. Haungs, The cosmic-ray spectrum in the PeV to EeV energy range, Advances in Space Research, https://doi.org/10.1016/j.asr.2024.06.053

Supernova remnants are generally believed to be a source for galactic cosmic rays from about 10 TeV up to around 1 PeV with acceleration of the particle by the first order Fermi mechanism (Fermi, 1949). The cosmic ray particles gain their final energy by many interactions each with a small increase of the energy emitted by supernova explosions. The maximum attainable energy of charged particles is obtained by $E_{knee} \propto Z \cdot B \cdot R$, where Z is the cosmic ray particle charge, B and R are the magnetic field strength and the size of the acceleration region, respectively.

In the energy range at around 10^{18} eV, an important feature is the ankle, which is characterized by a flattening of the spectrum. Cosmic rays above ankle are most probable of extra-galactic origin, so that in this energy range a breakdown of the heavy component and a transition from a galactic to an extra-galactic dominated composition are expected (Hillas, 2005; Berezinsky et al., 2006; Ginzburg, 1979).

Observations performed by various experiments using different measurements techniques in the energy interval of 10^{15} to 10^{18} eV showed the existence of individual knees in the spectra of the light, the intermediate and the heavy mass groups of cosmic rays.

In this review, the following experiments presently under consideration are discussed. KASCADE-Grande (Navarra et al., 2004) measured the electromagnetic components with scintillation detectors and in addition low energy muons of the air showers with shielded scintillators. IceTop (Abbasi et al., 2013) uses the Ice-Cherenkov tanks to measure air showers and has a possibility to include the detection of high-energy muons with IceCube. The Telescope Array Low-Energy Extension (TALE) (Abbasi et al., 2018) experiment detects low-energy cosmic rays in the PeV energy range using atmospheric fluorescence detectors, which are also sensitive to the directed Cherenkov radiation produced by shower particles. Their results on the all-particle energy spectrum with mass composition are discussed. Afterward, a brief discussions on the implication on the results and open questions are followed.

2. All-particle energy spectrum

2.1. Around the knee region

After the discovery of the knee of cosmic rays, many experimental observations as well as theoretical studies have been performed. However, the origin of the knee remains still controversial.

Most theories plausibly explain the steepening of the spectrum by the break of galactic acceleration mechanisms of the cosmic rays (Hillas, 2005) or by the limit on their confinement during propagating through the galaxy (Ptuskin et al., 1993). Another possibility is related to the nature of hadronic interactions. In the former models, the knee positions for different cosmic rays depend on their atomic number Z, named rigidity dependency, the latter favour spectral changes proportional to the number of nucleons A.

Despite, in any of these models, light particles drop out of the spectrum first, so that the energy position of the knee is expected to vary from light to heavy elements, i.e. protons would steepen first, then helium, then CNO. Following that, the heaviest element to be steepened would be the iron (Blümer et al., 2009; Haungs et al., 2003).

In various experiments, the knee feature at around $3 - 4 \cdot 10^{15}$ eV is observed in the hadronic, muonic and electromagnetic components (Antoni et al., 2005; Amenomori et al., 2008; Varsi et al., 2022), as well as in Cherenkov-light measurements (Budnev et al., 2020) and it is consistent within the experimental uncertainties. However, a general agreement does not exist yet, namely, on the chemical mass component for the knee in the spectrum.

2.2. The iron-knee

According to the rigidity dependency, the position of the knee is predicted to vary from light to heavy elements, so that the iron represented with the heaviest element is expected to be steepened at around 10^{17} eV following previous KASCADE observations (Antoni et al., 2005). Therefore, an understanding of the origin of the steepening around 10^{17} eV in the spectrum in terms of mass group separation is important.

KASCADE-Grande is one of the main experiments for this purpose. The data of KASCADE-Grande are considered only at energies $> 10^{16.2}$ eV to avoid bias effects due to different thresholds for different primaries at larger zenith angles. The study is performed subdividing the measured data in two samples, which are defined as heavy and light mass groups based on the correlation between the size of the charged particles (N_{ch}) and muon numbers (N_{μ}) on an event-by-event basis. A detailed description on the analysis can be found in Ref. (Apel et al., 2011). The result from the data set of the heavy element group shows a distinct knee-like feature around 10^{17} eV (Apel et al., 2011). This knee-like feature of the all-particle spectrum as well as of the spectrum of heavy primaries observed by KASCADE-Grande is confirmed by other experiments such as IceTop (Aartsen et al., 2019), TALE (Abbasi et al., 2018) and the Pierre Auger Observatory (Abreu et al., 2021).

Fig. 1 presents the all-particle energy spectra from various experiments EAS-TOP, KASCADE, KASCADE-Grande, IceCube/IceTop, Pierre Auger Observatory and Telescope Array. Recent results from KASCADE-Grande (Kang et al., 2023) show the spectra based on the different post-LHC interaction models, QGSJET-II-04 (Ostapchenko, 2011), EPOS-LHC (Pierog et al., 2015) and SIBYLL 2.3d (Riehn et al., 2020). It is interesting to note that the KASCADE-Grande results show relatively

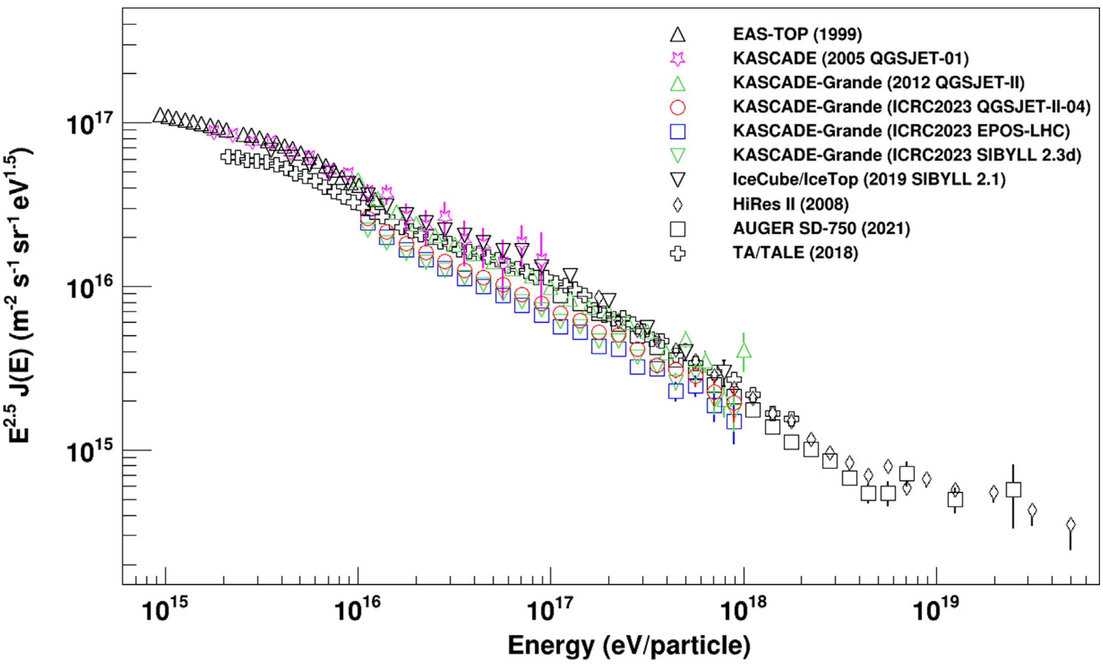

Fig. 1. All-particle energy spectrum from various air-shower experiments: EAS-TOP (Aglietta et al., 1999), KASCADE (Antoni et al., 2005), KASCADE-Grande (Apel et al., 2012), IceCube/IceTop (Aartsen et al., 2019), Pierre Auger Observatory (Abreu et al., 2021), Telescope Array (Abbasi et al., 2018).

small dependencies among the post-LHC hadronic interaction models in use. However, with regard to the absolute flux, there is for KASCADE-Grande an up to 20% lower flux compared to the other measurements. This might be due to the measurements close to sea level, for experiments located at higher altitudes, the variations caused by reconstructions based on different hadronic interaction models seems to be smaller. Moreover, as KASCADE-Grande measures the total number of electrons and muons, separately, these differences are related to the absolute normalization of the energy scale by the various models.

IceCube/IceTop announced the measurements of all-particle spectrum and energy spectra for different primary mass groups, by combining the events measured by IceTop and the in-ice detector of IceCube in coincidence (Aartsen et al., 2019). The resulting spectra derived from three years of IceCube/IceTop data confirmed two features, the knee around 5 PeV and a second knee around 100 PeV.

Recently, the Pierre Auger Observatory reported the all-particle energy spectrum down to around 100 PeV (Abreu et al., 2021). This observation suggests that the second knee is not a sharp feature, and this feature is linked to a softening of the spectrum of heavy primaries beginning at around 10^{17} eV by the KASCADE-Grande experiment.

All experiments operate at different observation levels, use different analysis techniques and different hadronic interaction models to interpret their data, nevertheless, a good agreement between the results of different experiments is shown in the energy range of PeV to EeV. At $\sim 10^{18}$ eV, the KASCADE-Grande result is statistically in agreement with the result of Pierre Auger Observatory.

2.3. Hardening above the iron-knee

Following to results from the KASCADE-Grande experiment, a knee-like feature in the all-particle energy spectrum of cosmic rays is observed at $10^{16.92}$ eV (Apel et al., 2011). It is due to the steepening in the flux of heavy primaries. The combined spectrum of light and intermediate mass components was found to be compatible with a simple power law. However, the spectral feature just above 10^{17} eV shows a change of the slope, namely, a hardening or ankle-like feature of light primaries.

In KASCADE-Grande, for such a spectral feature, a more detailed investigation is performed by means of data with higher statistics. To obtain increased statistics, a larger fiducial area was used and the selection criteria for the enhancement of light primaries is optimized as well. Detailed analysis procedures is described in Ref. (Apel et al., 2013). This result is based on the N_{ch}-N_{μ} technique by calibrating with the hadronic interaction model of QGSJET-II. A hardening, i.e. an ankle-like feature is visible in the spectrum of the light primaries, where a change of the spectral slope from -3.25 to -2.79 is observed at an energy of $10^{17.08}$ eV. This might imply that the transition from galactic to extra-galactic origin starts already in this energy region.

In astrophysical models, the transition region from galactic to extra-galactic origin of cosmic rays is generally expected in the energy range from 10^{17} to 10^{19} eV. In addition, one should expect a hardening of the proton or light primaries components of the cosmic ray spectrum to take place below or around 10^{18} eV, since the onset of the extra-galactic contribution is dominated by light primaries.

3. Mass composition

The mass composition of cosmic rays is one of the most important studies to understand the origin of cosmic rays and the physical processes at the sources. However, this has to be determined by the measurements of the properties of the atmospheric showers and has an large influence by the systematic uncertainties related to the hadronic interaction models. Generally, in ground-based experiments, elemental composition can be investigated in terms of the individual spectra, e.g. "light" and "heavy" components or the evolution of $< \ln A >$ with energy.

Recent results of the energy spectra of heavy (Si + Fe) and light (H + He + CNO) mass groups measured by KASCADE-Grande (Kang et al., 2023) are shown in Fig. 2. They are reconstructed by means of the relation $E(N_{ch})$ for two separated samples, using the model-dependent energy calibration function. The spectrum of heavy components confirms the knee-like structure at around $10^{16.7}$ eV, where the power spectral index changes from -2.7 to -3.3. In the spectrum of light primaries, a hardening feature above about $10^{16.5}$ eV is also observed and the spectral slope changes smoothly.

The energy spectra of QGSJET-II-04 only is displayed in Fig. 2. Details about the individual energy spectra determined on basis of EPOS-LHC and SIBYLL 2.3d can be found in Ref. (Kang et al., 2023). The energy spectra of QGSJET-II-04 and SIBYLL 2.3d show a very similar tendency, whereas the total flux of EPOS-LHC is shifted by about 10% due to the different ratio of N_{ch}/N_{μ}. In particular, the EPOS-LHC model predicts more muons than the other post-LHC models, so that the data interpretation leads to a more light composition. In general, the light component sample in KASCADE-Grande is more abundant due to the separation around the CNO mass group. The muon content might also affect some difference of absolute abundances. However, all spectra show similar characteristics of the energy spectrum for all models.

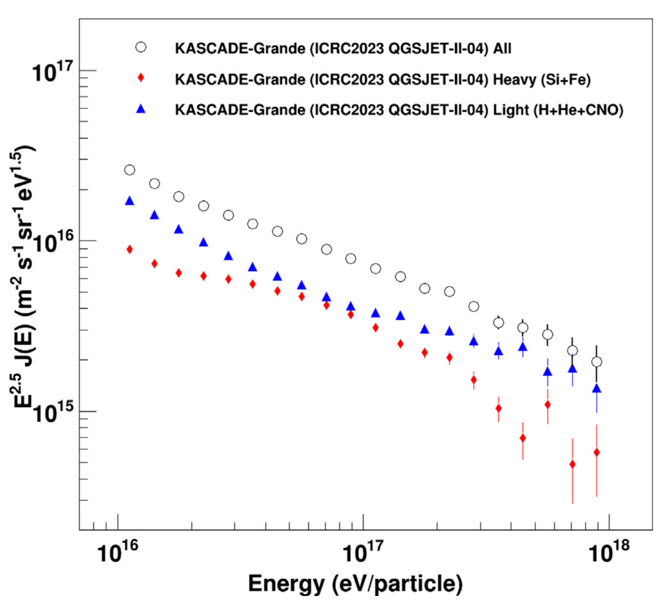

Fig. 2. The spectra of heavy (red rhombus) and light (blue triangle) mass groups measured by KASCADE-Grande (Kang et al., 2023.) are displayed. (For interpretation of the references to colour in this figure legend, the reader is referred to the web version of this article.)

IceCube presented the mean logarithmic mass $< \ln A >$, which is derived by the individual fractions from the mass output of the neural network technique. The distribution of the mean mass shows that composition becomes heavier with increasing energy up to 10^{17} eV (Aartsen et al., 2019). In addition, the composition spectra from different experiments agree with each other, except the proton spectrum between IceTop and KASCADE. This could be related to the different handling of the intermediate mass groups, which are strongly correlated with other mass components, in particular for the absolute abundance of the primary mass group. Another effect could be due to the different observation level.

4. Astrophysical interpretations

Various experiments indicate that the knee, the most conspicuous characteristics in the all-particle energy spectrum is caused mainly by a break in the spectra for the light primaries, where the mean mass of cosmic rays increases in this region. However, the interpretation of the knee of the energy spectrum of cosmic rays is still under discussion, in particular, if there are more than one knee for individual primaries, e.g. due to various sources or source populations with different maximum acceleration energies (ARGO (Bartoli et al., 2015), LHAASO (You et al., 2023), GRAPES-3 (Varsi et al., 2024)).

One of the most general interpretation for the origin of the knee is that the bulk of cosmic rays is assumed to be accelerated in the strong shock fronts of SNRs (Fermi, 1949), in which the spectrum at the source shows a pronounced break. The observed knee produced by the steepening of protons is at an energy of $E_{knee} \sim 4 \cdot 10^{15}$ eV, which is possibly close to the size ($\sim$ parsec) of SNRs.

The maximum attainable energy of cosmic ray particles has a rigidity dependency (Hillas, 2005), so that the energy position of the knees presents a sequence of steepening of different nuclei with increasing Z. The steepening of iron is thus easily expected at energy of $26 \times E_{knee}$. The first evidence for that has been seen by KASCADE-Grande measurement with a knee-like structure of the heavy primary spectrum (Apel et al., 2011). This result supports the structures of the knee region caused as a rigidity dependent feature of the composition.

The acceleration mechanism, i.e. the acceleration of particles in γ-ray bursts is also debated. The γ-ray bursts associated with supernova explosions are proposed to accelerate cosmic rays from about 10^{14} eV up to the highest energies. The propagation effects of the cosmic rays is taken into account in this approach, and the knee caused by the leakage of particles from the galaxy leads to rigidity dependent behavior.

Hillas proposed the rigidity dependency of the flux for individual elements. In this model, the spectra are reconstructed with rigidity dependent knee feature at higher energies. By means of the properties of accelerated cosmic rays in SNRs and the fluxes derived by KASCADE, Hillas obtained the all-particles flux, which is not sufficient to describe the measured flux at energy above 10^{16} eV. For this gap, Hillas proposed a second galactic component, which he named as 'component B'. An extra-galactic component becomes significant at energies above 10^{19} eV. The flux of galactic cosmic rays extends to higher energies in this case, therefore, a dominated contribution of the extra-galactic component is expected only above 10^{18} eV.

The transition between galactic and extra-galactic cosmic rays occurs most probably at energies around 10^{17} and 10^{18} eV. The transition is an important feature since breaks in all-particle energy spectrum and in composition are associated with the particle production mechanism, the source contribution, as well as their propagation.

In the model of Berezinsky (Berezinsky et al., 2006), using the model for extra-galactic ultra-high energy cosmic rays and the observed all-particle cosmic ray spectrum by Akeno and AGASA experiments, the galactic spectrum of iron nuclei in the energy range of $10^{17} - 10^{18}$ eV is calculated. In the transition region of this model, spectra of only galactic iron nuclei and of extra-galactic protons are mainly taken into account. The predicted flux by Berezinsky at lower energies is well agreeable with results of the KASCADE data. The transition from galactic to extra-galactic cosmic rays is obviously seen in spectra of protons and iron nuclei. Above $10^{17.5}$ eV, the spectrum can be described by a proton dominated composition.

5. Summary

We discussed briefly the all-particle energy spectra measured by different ground-based experiments in the PeV to EeV primary energy range. Several features have been observed in the energy spectrum of cosmic rays: The first dominant feature, the knee, in the all-particle energy spectrum of cosmic rays is a softening of the spectrum at an energy of about $3 \cdot 10^{15}$ eV, which is mainly caused by the light components of cosmic rays. A knee-like feature in the spectrum of the heavy primaries of cosmic rays, as well as in the all-particle energy spectrum, is observed at around $8 - 15 \cdot 10^{16}$ eV. At around 10^{17} eV, an ankle-like structure, i.e. a remarkable hardening, in the energy spectrum of light components of cosmic rays is observed. This implies that the transition from galactic to extra-galactic origin of cosmic rays might occur already in this energy region.

With respect to the mass composition, the findings of KASCADE-Grande, IceCube/IceTop and Auger are qualitatively in agreement with each other. Though a large uncertainty in the absolute flux/composition, a common general trend is revealed that composition gets heavier through the knee region and becomes lighter approaching the ankle.

By means of different hadronic interaction models (post-LHC), there is a shift in the absolute energy scale of the spectra, but the shape of the spectrum with its structures remains. Nevertheless, improving the uncertainty in the hadronic interaction models used to the shower development is expected. Up to today the various hadronic interaction models fail to give a consistent picture of reconstructed primary energy and mass of measured extensive air showers for different observables (measured shower components) and/or different observation altitudes. The most obvious way to solve this problem is to analyse the data from several experiments with the same simulations (Schröder et al., 2019), and to use improved accelerator measurements, for example with a dedicated forward detector (Soldin, 2023). It would help if the experiments were to make their (also archived) air-shower data freely accessible, as the KASCADE-Grande experiment has done with the KCDC portal (Haungs et al., 2018).

However, in addition, further details are still required to be clarified by future and more sensitive experiments, such as, whether the origin of the second knee stems from, or the knee energies of different elements depend on their charge or their mass. To enable a better understanding of these open questions, for instance, in IceCube further analyses are under investigation: more years of experimental data are available and more intermediate elements of cosmic rays are simulated. Furthermore, an investigation of new composition-sensitive parameters is currently under development. Moreover, an enhancement of the surface array IceTop with a multi-detector array of scintillation detectors and radio antennas is planned (Aartsen et al., 2021).

Declaration of competing interest

The authors declare that they have no known competing financial interests or personal relationships that could have appeared to influence the work reported in this paper.

References

Aartsen, M.G., Abbasi, R., Ackermann, M., et al.IceCube, 2021. IceCube-Gen2: the window to the extreme universe. J. Phys. G: Nucl. Part. Phys. 48, 060501. https://doi.org/10.1088/1361-6471/abbd48.

Aartsen, M.G., Ackermann, M., Adams, J., et al.IceCube, 2019. Cosmic ray spectrum and composition from PeV to EeV using 3 years of data from IceTop and IceCube. Phys. Rev. D 100, 082002. https://doi.org/10.1103/PhysRevD.100.082002.

Abbasi, R., Abdou, Y., Ackermann, M., et al.IceCube, 2013. IceTop: The surface component of IceCube. Nucl. Instr. and Meth. A 700, 188–220. https://doi.org/10.1016/j.nima.2012.10.067.

Abbasi, R.U., Abe, M., Abu-Zayyad, T. et al. (Telescope Array), 2018. The cosmic-ray energy spectrum between 2 PeV and 2 EeV observed with the TALE detector in monocular mode. Astrophys. J., 865, 74 (18pp). doi:10.3847/1538-4357/aada05.

Abreu, P., Aglietta, M., Albury, J.M., et al.Pierre Auger, 2021. The energy spectrum of cosmic rays beyond the turn-down around 10^{17} eV as measured with the surface detector of the Pierre Auger Observatory. Eur. Phys. J. C 81, 966. https://doi.org/10.1140/epjc/s10052-021-09700-w.

Aglietta, M., Alessandro, B., Antonioli, P., et al.ESA-TOP, 1999. The EAS size spectrum and the cosmic ray energy spectrum in the region $10^{15} - 10^{16}$ eV. Astropart. Phys. 10, 1–9. https://doi.org/10.1016/S0927-6505(98)00035-8.

Amenomori, M., Bi, X.J., Chen, D., et al.TIBET-III, 2008. The all-particle spectrum of primary cosmic rays in the wide energy range from 10^{14} eV to 10^{17} eV observed with the Tibet-III air-shower array. Astrophys. J. 678, 1165–1179. https://doi.org/10.1086/529514.

Antoni, T., Apel, W.D., Badea, A.F., et al.KASCADE, 2005. KASCADE measurements of energy spectra for elemental groups of cosmic rays: Results and open problems. Astropart. Phys. 24, 1–25. https://doi.org/10.1016/j.astropartphys.2005.04.001.

Apel, W.D., Arteaga-Velázquez, J.C., Bekk, K., et al.KASCADE-Grande, 2011. Kneelike Structure in the Spectrum of the Heavy Component of Cosmic Rays Observed with KASCADE-Grande. Phys. Rev. Lett. 107, 171104. https://doi.org/10.1103/PhysRevLett.107.171104.

Apel, W.D., Arteaga-Velázquez, J.C., Bekk, K., et al.KASCADE-Grande, 2012. The spectrum of high-energy cosmic rays measured with KASCADE-Grande. Astropart. Phys. 36, 183–194. https://doi.org/10.1016/j.astropartphys.2012.05.023.

Apel, W.D., Arteaga-Velázquez, J.C., Bekk, K., et al.KASCADE-Grande, 2013. Ankle-like feature in the energy spectrum of light elements of cosmic rays observed with KASCADE-Grande. Phys. Rev. D 87, 081101. https://doi.org/10.1103/PhysRevD.87.081101.

Bartoli, B., Bernardini, P., Bi, X.J., et al.ARGO-YBJ, 2015. Cosmic ray proton plus helium energy spectrum measured by the ARGO-YBJ experiment in the energy range 3–300 TeV. Phys. Rev. D 91, 112017. https://doi.org/10.1103/PhysRevD.91.112017.

Berezinsky, V., Gazizov, A., Grigorieva, S., 2006. On astrophysical solution to ultrahigh energy cosmic rays. Phys. Rev. D 74, 043005. https://doi.org/10.1103/PhysRevD.74.043005.

Blümer, J., Engel, R., Hörandel, J.R., 2009. Cosmic Rays from the Knee to the Highest Energies. Prog. Part. Nucl. Phys. 63, 293–338. https://doi.org/10.1016/j.ppnp.2009.05.002.

Budnev, N.M., Chiavassa, A., Gress, O.A., et al.TUNKA, 2020. The primary cosmic-ray energy spectrum measured with the Tunka-133 array. Astropart. Phys. 117, 102406. https://doi.org/10.1016/j.astropartphys.2019.102406.

Fermi, E., 1949. On the Origin of the Cosmic Radiation. Phys. Rev. 75, 1169. https://doi.org/10.1103/PhysRev.75.1169.

Ginzburg, V.L., 1979. Theoretical Physics and Astrophysics, (1st ed.). Pergamon Press Ltd., Oxford, pp. 343–387.

Haungs, A., Kang, D., Schoo, S., et al., 2018. The KASCADE Cosmic-ray Data Centre KCDC: Granting Open Access to Astroparticle Physics Research Data. Eur. Phys. J. C 78 (9), 741. https://doi.org/10.1140/epjc/s10052-018-6221-2, arXiv:1806.05493.

Haungs, A., Rebel, H., Roth, M., 2003. Energy spectrum and mass composition of high-energy cosmic rays. Rep. Prog. Phys. 66 (7), 1145–1206. https://doi.org/10.1088/0034-4885/66/7/202.

Hillas, A.M., 2005. Can diffusive shock acceleration in supernova remnants account for high-energy galactic cosmic rays? J. Phys. G: Nucl. Part. Phys. 31, R95–R131. https://doi.org/10.1088/0954-3899/31/5/R02.

Kang, D., Arteaga-Velázquez, J.C., Bertaina, M. et al. (KASCADE-Grande), 2023. Latest Analysis Results from the KASCADE-Grande Data. In Proceedings, 38th International Cosmic Ray Conference (ICRC2023), Nagoya, Japan 2023 (p. PoS(ICRC2023)307). doi:10.22323/1.444.0307. arXiv:2312.05054.

Navarra, G., Antoni, T., Apel, W.D., et al.KASCADE-Grande, 2004. KASCADE-Grande: A large acceptance, high-resolution cosmic-ray detector up to 10^{18} eV. Nucl. Instr. Meth. A 518, 207–209. https://doi.org/10.1016/j.nima.2003.10.061.

Ostapchenko, S., 2011. Monte Carlo treatment of hadronic interactions in enhanced Pomeron scheme: QGSJET-II model. Phys. Rev. D 83, 014018. https://doi.org/10.1103/PhysRevD.83.014018.

Pierog, T., Karpenko, I., Katzy, J.M., et al., 2015. EPOS LHC: Test of collective hadronization with data measured at the CERN Large Hadron Collider. Phys. Rev. C 92, 034906. https://doi.org/10.1103/PhysRevC.92.034906.

Ptuskin, V.S., Rogovaya, S.I., Zirakashvili, V.N., et al., 1993. Diffusion and drift of very high energy cosmic rays in galactic magnetic fields. Astron. Astroph. 268, 726–735.

Riehn, F., Engel, R., Fedynitch, A. et al., 2020. Hadronic interaction model SIBYLL 2.3d and extensive air showers. Phys. Rev. D, 102, 063002. doi:10.1103/PhysRevD.102.063002.

Schröder, F.G., AbuZayyad, T., Anchordoqui, L., et al., 2019. High-Energy Galactic Cosmic Rays (Astro2020 Science White Paper). Bull. Am. Astron. Soc. 51, 131. https://doi.org/10.48550/arXiv.1903.07713, arXiv:1903.07713.

Soldin, D., 2023. Astroparticle Physics with the Forward Physics Facility at the High-Luminosity LHC. In: Proceedings, 38th International Cosmic Ray Conference (ICRC2023), Nagoya, Japan 2023 (p. PoS (ICRC2023)327). doi:10.22323/1.444.0327. arXiv:2308.09079.

Varsi, F., Ahmad, S., Chakraborty, M. et al. (GRAPES-3), 2022. Latest Results of Cosmic Ray Energy Spectrum and Composition Measurements From GRAPES-3 Experiment. In: Proceedings of the XXIV DAE-BRNS High Energy Physics Symposium, Jatni, India (pp. 649–654). volume 277. doi:10.1007/978-981-19-2354-8_118.

Varsi, F., Ahmad, S., Chakraborty, M., et al.GRAPES-3, 2024. Evidence of a Hardening in the Cosmic Ray Proton Spectrum at around 166 TeV Observed by the GRAPES-3 Experiment. Phys. Rev. Lett. 132, 051002. https://doi.org/10.1103/PhysRevLett.132.051002.

You, Z., Zhang, S., Yin, L. et al. (LHAASO), 2023. Measurement of the cosmic ray proton spectrum around the knee region with LHAASO. In: Proceedings, 38th International Cosmic Ray Conference (ICRC2023), Nagoya, Japan 2023 (p. PoS(ICRC2023)423). doi:10.22323/1.444.0423.